albedo is $j = 12.6 \times 10^{-4}$ s^{-1}, 17% (24%) lower than our value.

5. Summary and Conclusions

A UV absorption spectrum of pure gaseous HONO has been obtained at a spectral resolution of 0.1 nm, by careful subtraction of NO_2 from composite spectra of highly diluted HONO/NO/NO_2/H_2O mixtures in nitrogen. Existing uncertainties in absolute absorption cross sections could be reduced to approximately ±5% or $\pm 5 \times 10^{-21}$ cm^2, whichever is greater, in the investigated spectral range. Owing to recent theoretical work, the photochemistry of HONO, particularly the continuous nature of the spectrum and the line shapes of bands, are now well established. Salient features of the spectrum have been reproduced by a synthetic spectrum composed of Lorentzian bands of the trans and cis rotamers, which form progressions of the upper state N=O stretching vibration, υ_2'. Deconvolution of the spectrum into progressions of the trans and cis rotamers yields an estimate of the equilibrium constant $N_{trans}/N_{cis} = K$, corresponding to an energy difference $\Delta E = -646$ cal mol^{-1} (2700 J mol^{-1}) between the rotamers, in good agreement with a recent theoretical estimate.

Acknowledgment. This work, part of which has been presented at the EUROTRAC Symposium 1990 in Garmisch-Partenkirchen, was supported by the European Economic Community and by the German BMFT. A financial contribution of Fonds der Chemischen Industrie to our computing and word processing system is gratefully acknowledged. We thank Silke Schweighoefer for valuable assistance.

A Molecular Dynamics Study of Pressure Effects on Solvation and Optical Spectra: The Ground and Excited States of Formaldehyde in Water

Mahfoud Belhadj, Douglas B. Kitchen, Karsten Krogh-Jespersen, and Ronald M. Levy*

Department of Chemistry, Rutgers University, New Brunswick, New Jersey 08904 *(Received: July 23, 1990)*

Molecular dynamics simulations of formaldehyde in liquid water have been carried out at high pressures (1 and 10 kbar). The results of three sets of simulations are reported corresponding to the equilibrium solvation of this model dipolar solute in the ground state ($^1A_1$), the first excited singlet state ($^1A''$), and the nonequilibrium solvation following a simulated electronic excitation. The high-pressure simulations are compared with the results at low pressure (1 bar) reported previously. The changes in the structure of the solvation shell of the ground-state species as the pressure is increased to 10 kbar are relatively small. In contrast, there are more substantial changes in the solvation structure of the excited-state species with increasing pressure. At low pressure, the solvation shell surrounding the $^1A''$ state is disordered relative to that of the ground state. High pressure induces the formation of a distinct solvation shell around the formyl oxygen in the excited state. The waters in the first solvation shell have rotated by 180°, however, with respect to their preferred orientation in the ground state. Because of compensating effects involving different atoms of the solute, the changes in the total solvation energies of the ground and excited states with pressure are small, leading to a small pressure-induced blue shift in the optical absorption. These results indicate that it is important to account for the extended shape and charge distribution of the solute and the molecular nature of the solvation shell when considering pressure-induced effects on optical spectra. The nonequilibrium solvation dynamics corresponding to a laser-induced excitation is simulated by following 80 trajectories which start from different configurations on the ground-state surface. At high pressure, the rotational relaxation of waters in the first solvation shell is an order of magnitude slower than the solvent response at low pressure. The use of simulations to aid in developing molecular models for "pressure tuning spectroscopy" experiments is discussed.

Introduction

The analysis of solvent effects on optical absorption bands is a classical method that has long been used to study the energetics and dynamics of solvation.[1-5] In the simplest description of the process, an optical excitation leads to a sudden charge redistribution within the solute; the differential solvation between the two electronic states results in an absorption line shift. After excitation, the solute and solvent begin to relax and this leads to a time-dependent fluorescence shift. The intimate relationship that exists between effects observed in time-resolved fluorescence experiments and electron transfer has been discussed by several authors.[2,5-9] Several lines of theoretical analysis point to the important role played by the first solvation shell in the solvent response following an optical excitation.[7-15] We have been engaged in a series of calculations on the effects of solvation on the electronic and spectral properties of model solute–solvent systems.[14a-d] In a recent communication, we reported the results of molecular dynamics simulations of the time-resolved fluorescence from the first excited singlet state ($^1A''$) of a model dipolar solute, formaldehyde, in water.[14d] In this paper we extend this work to simulations of high-pressure effects on the solvation of the ground

(1) Bayliss, N. J. *J. Chem. Phys.* **1950**, *18*, 292.
(2) Marcus, R. A. *J. Chem. Phys.* **1965**, *43*, 1261.
(3) Okamoto, B. Y.; Drickamer, H. G. *Proc. Natl. Acad. Sci. U.S.A.* **1974**, *71*, 2671.
(4) Mataga, N.; Kubota, T. *Molecular Interactions and Electronic Spectra*; Marcel Dekker: New York, 1970.
(5) Fleming, G. R. *Chemical Applications of Ultrafast Spectroscopy*; Oxford University Press: New York, 1986.
(6) Van der Zwan, G.; Hynes, J. T. *J. Phys. Chem.* **1985**, *89*, 4181.
(7) Wolynes, P. G. *J. Chem. Phys.* **1987**, *86*, 5133.
(8) Loring, R.; Yan, Y.; Mukamel, S. *J. Chem. Phys.* **1987**, *87*, 5841.
(9) Nichols, A.; Calef, D. *J. Chem. Phys.* **1988**, *89*, 3783.
(10) Karim, O.; Haymet, A. D.; Banet, M. J.; Simon, J. D. *J. Phys. Chem.* **1988**, *92*, 3391.
(11) Maroncelli, M.; Fleming, G. R. *J. Chem. Phys.* **1988**, *89*, 5044.
(12) Maroncelli, M.; MacInnis, J.; Fleming, G. *Science* **1989**, *24*, 1674.
(13) Chandra, A.; Bagchi, B. *J. Phys. Chem.* **1990**, *94*, 1874.
(14) (a) Blair, J. T.; Westbrook, J. D.; Levy, R. M.; Krogh-Jespersen, K. *Chem. Phys. Lett.* **1989**, *154*, 531. (b) Blair, J. T.; Krogh-Jespersen, K.; Levy, R. M. *J. Am. Chem. Soc.* **1989**, *111*, 6948. (c) Blair, J. T.; Levy, R. M.; Krogh-Jespersen, K. *Chem. Phys. Lett.* **1990**, *166*, 429. (d) Levy, R. M.; Kitchen, D. B.; Blair, J. T.; Krogh-Jespersen, K. *J. Phys. Chem.* **1990**, *94*, 4470.
(15) Debolt, S. E.; Kollman, P. A. *J. Am. Chem. Soc.*, in press.

0022-3654/91/2095-1082$02.50/0

and excited states of formaldehyde. Pressure-dependent studies of the optical spectrum of dissolved solutes can, in principle, provide a great deal of information about electronic structure and solute–solvent interactions.[16] Simulations can have a valuable role in separating intramolecular from intermolecular effects. Molecular interpretations of pressure-dependent spectral changes in water are particularly difficult; large pressure-induced red shifts have been attributed to attractive intermolecular forces between solute and solvent molecules participating in hydrogen bonds.[17] Available evidence from simulations suggests that, for neat liquid water at least, the effect of pressure (at 10 kbar) is actually to decrease the strength of individual hydrogen bonds between water molecules, while the number of hydrogen bonds to each water molecule increases.[18] For liquid methanol, the application of pressures to 15 kbar does not appear to increase the strength or number of hydrogen bonds.[19] For model solutes like formaldehyde which undergo a large change in their dipole moment and hydrogen-bonding properties upon excitation, it is unclear how pressures will affect the relative solvation by water of the ground versus the excited state and the hydrogen bonding between solute and solvent.

Formaldehyde serves as a prototypical molecule to study the solvation and spectroscopic properties of the carbonyl group. The $n \rightarrow \pi^*$ transition of the carbonyl group involves the promotion of an electron from an in-plane oxygen lone pair, oriented perpendicular to the C=O axis and almost exclusively of O(2p) character, into the out-of-plane π^* C=O orbital that has its largest coefficient on the carbon atom.[20] The transition causes a large reduction in the dipole moment, from 2.33 D (ground state) to 1.57 D (excited state).[21,22] Classical molecular dynamics and mixed classical/quantum simulations of ground-state formaldehyde in water at low pressure showed structured binding to the carbonyl oxygen by several water molecules.[14] Additional simulations of the solvated molecule using atomic partial charges corresponding to the excited-state species were carried out. Analysis of solute–solvent radial and angular distribution functions with solvent equilibrated around the excited state indicates a nearly complete loss of the structured solvation shell. The time-resolved fluorescence at low pressure was simulated.[14d] The fluorescence shift and solvation were found to relax nonexponentially on a very fast time scale, with the major portion of the relaxation occurring within 100 fs. The relaxation was dominated by changes in the structure of the first solvation shell. In this communication we compare the solvation structure, energetics, and dynamics of the ground and excited states of formaldehyde at 1 and 10 kbar with the low-pressure results presented previously.[14b,d]

Method

Molecular dynamics simulations of a formaldehyde solute molecule in a cubic box of 209 water molecules were carried out in the NPT ensemble using the IMPACT program.[23] The equations of motion were integrated by using Andersen's RATTLE algorithm[24] with a time step of 1 fs. Periodic boundary conditions were employed, with a spherical cutoff applied to the nonbonded interactions at 7.5 Å. Constant temperature and pressure conditions were maintained by using the "coupling to an external bath" method of Berendsen et al.[25] The relaxation times for the temperature and pressure scaling were set to 10 fs. Results from simulations at three different pressures, 1 bar, 1 kbar, and 10 kbar, are reported. Each simulation was continued for 20 ps. The average temperature in these simulations was 298 K. The molecular mechanics parameters employed for ground and excited states of formaldehyde were the same as those used in our previous work.[14c] For water, the SPC model was used.[26] The average volume of the simulation box was 6.49×10^4 Å^3 at 1 bar, 6.29×10^4 Å^3 at 1 kbar, and 5.17×10^4 Å^3 at 10 kbar. This corresponds to a ~25% increase in density as the pressure is increased from 1 bar to 10 kbar; the results are in reasonable accord with experiment for which the observed increase is 22% at 340 K.[27]

The equilibrium geometry of ground state (S_0) formaldehyde is planar (C_{2v} symmetry, $^1A_1$), whereas the structurally relaxed, excited singlet state (S_1) is pyramidal around the C atom (C_s symmetry, $^1A''$). Separate equilibrium molecular dynamics simulations with formaldehyde in the ground and excited state have been completed at 1 and 10 kbar. Solute–solvent radial and angular distribution functions and solvation energies have been computed from each of the equilibrium simulations. In addition, high-pressure nonequilibrium solvation simulations have been carried out using the method described previously.[14c] The vertical excitation of formaldehyde is simulated by instantaneously switching the formaldehyde charges and force constants from $^1A_1$ ground-state values to those corresponding to the $^1A''$ excited state. The system is then propagated forward in time by integrating the equations of motion. Eighty such trajectories corresponding to different initial conditions were calculated and averaged. The initial coordinates and velocities for these nonequilibrium trajectories were generated from equally spaced points sampled from the simulation of ground-state formaldehyde in water.

Results and Discussion

A. Structure and Dynamics of Water at High Pressure. The pressure dependence of the water O–O and O–H radial distribution functions is shown in Figure 1, a and b. The radial distribution functions were calculated by averaging over the solvent molecules in simulations which also contained a single solute molecule; the results are dominated by the bulk water properties. At 1 bar, the characteristic features of the water O–O radial distribution function are observed. There is a large maximum at 2.8 Å, a minimum at 3.4 Å, followed by a second smaller maximum at ~4.4 Å.[26,28] The O–O radial distribution function is unchanged at 1 kbar. However, significant changes are evident in the O–O radial distribution function at 10 kbar. The height of the first peak has decreased and moved in slightly, but the first peak is also substantially broadened at high pressure. Whereas at lower pressures (1 bar and 1 kbar) a maximum in the radial distribution function corresponding to the second peak is observed at ~4.4 Å, a minimum is observed in the radial distribution function at this position at 10 kbar. The changes in the O–H radial distribution, shown in Figure 1b, are smaller than those in the O–O distribution function. The first peak in the O–H radial distribution function decreases somewhat in intensity, and the second peak moves in slightly. Also, there is a more pronounced third peak in the O–H distribution function at ~5.7 Å in the high-pressure (10 kbar) simulation. The water–water hydrogen bond angular distribution functions as a function of θ (the O–H_1–O angle) are shown in Figure 1c. At low pressure there is a pronounced peak in the distribution function at $\cos\theta = -1$ corresponding to a linear hydrogen bond. The second broader peak at $\cos\theta \sim +0.6$ corresponds to the angle formed by the "other" hydrogen of the donor water molecule, i.e., the O–H_2–O angle. As the pressure is increased, the hydrogen bonds become more bent. This is reflected in the much broader hydrogen bond angle distribution at 10 kbar (Figure 1c). Similar pressure-dependent

(16) van Eldik, R., Jonas, J., Eds. *High Pressure Chemistry and Biochemistry*; NATO ASI Series 197; D. Reidel: Dordrecht, Holland, 1987.
(17) Lewis, N. A.; Obeng, Y. S.; Taveras, D. V.; van Eldik, R. *J. Am. Chem. Soc.* **1989**, *111*, 924.
(18) Madura, J.; Pettitt, M. *Mol. Phys.* **1988**, *64*, 325.
(19) Jorgensen, W. L.; Ibrahim, M. *J. Am. Chem. Soc.* **1982**, *104*, 373.
(20) Streitweiser, A.; Kohler, B. J. *J. Am. Chem. Soc.* **1988**, *110*, 3769.
(21) Jones, V. T.; Coon, J. B. *J. Mol. Spectrosc.* **1969**, *31*, 137.
(22) Buckingham, A. D.; Ramsey, D. A.; Tyrell, J. *Can. J. Phys.* **1970**, *48*, 1242.
(23) Bassolino, D. A.; Hirata, F.; Kitchen, D. B.; Kominos, D.; Pardi, A.; Levy, R. M. *Int. J. Supercomput. Appl.* **1988**, *28*, 41.
(24) Andersen, H. C. *J. Comput. Phys.* **1983**, *52*, 24.
(25) Berendsen, H. J. C.; Postma, J. P. M.; van Gunsteren, W. F.; DiNola, A.; Haak, J. R. *J. Chem. Phys.* **1984**, *81*, 3684.
(26) Berendsen, H. J. C.; Postma, J. P. M.; van Gunsteren, W. F.; Hermans, J. In *Intermolecular Forces*; Pullman, B., Ed.; Reidel: Dordrecht, 1981; p 331.
(27) Haar, L.; Gallagher, J. S.; Kell, G. S. *NBS/NRC Steam Tables*; Hemisphere Press: New York, 1984.
(28) Jorgensen, W. L.; Chandrasekhar, J.; Madura, J.; Impey, W.; Klein, M. *J. Chem. Phys.* **1983**, *79*, 926.

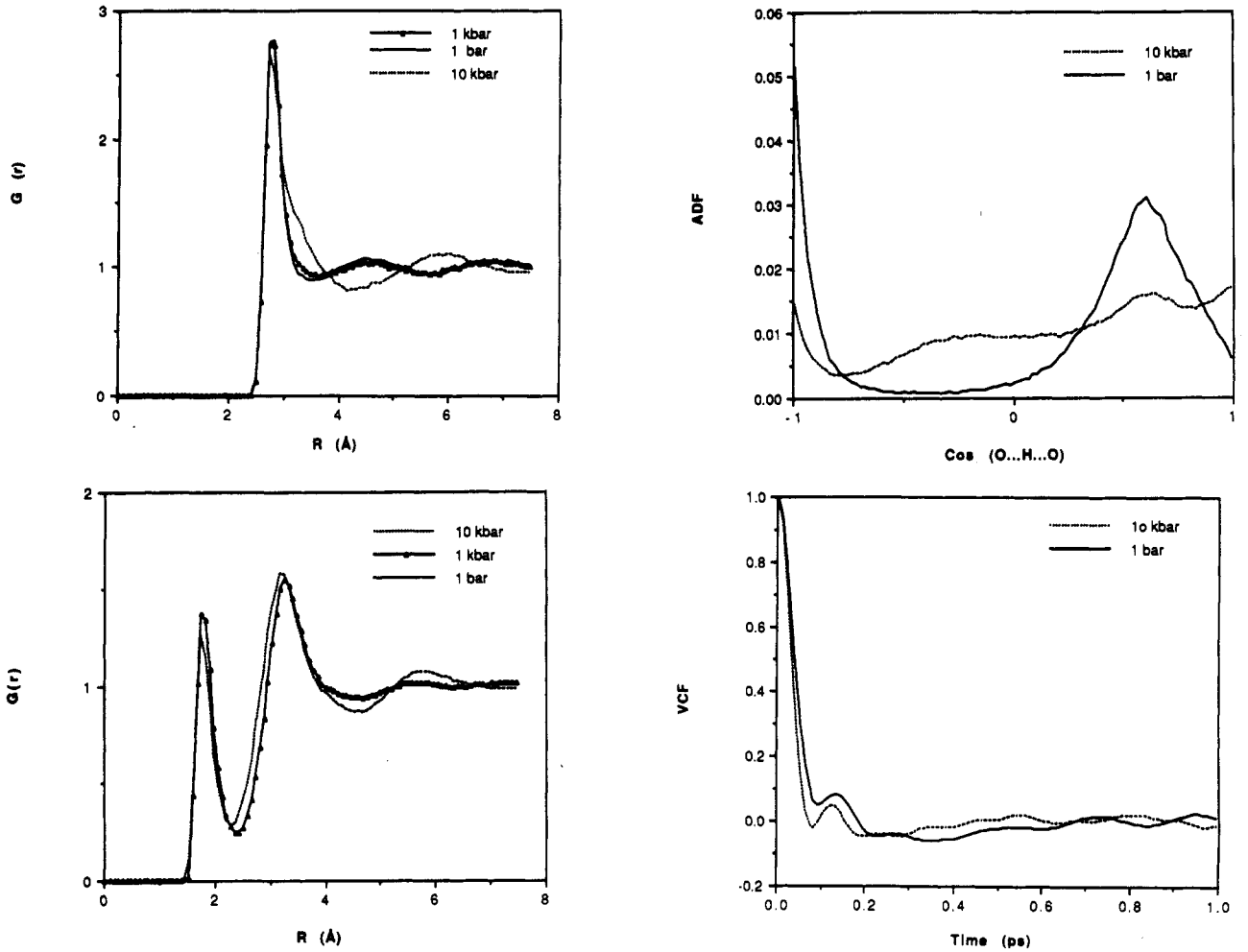

Figure 1. Water–water correlation functions: (a, upper left) oxygen–oxygen radial distribution function at 1 bar, 1 kbar, and 10 kbar; (b, lower left) oxygen–hydrogen radial distribution function at 1 bar, 1 kbar, and 10 kbar; (c, upper right) oxygen–hydrogen–oxygen angular distribution function for nearest-neighbor water molecules at 1 bar and 10 kbar; (d, lower right) center of mass velocity correlations function 1 bar and 10 kbar.

structural changes have also been reported in recent computer studies of TIP4P water at high pressure.[18,29] These authors have compared the simulated radial distribution functions corresponding to those probed in neutron-scattering experiments with experimental results up to 10 kbar and found good agreement between the experimental and simulated data. The structural analysis, together with an energetic analysis carried out by Madura et al.,[18] leads to a picture in which very little change occurs in the *local* tetrahedral structure of water as the pressure is increased to 10 kbar. Instead, the decrease in volume at increased pressures is achieved by increasing the packing efficiency between non-hydrogen-bonded neighbors. This corresponds to a filling in of the tetrahedral faces by next nearest neighbors to form interpenetrating hydrogen bond networks similar to what is observed for some forms of high-pressure ice.[18,29]

We have evaluated the pressure dependence of the water velocity correlation function and the diffusion coefficient. The results are shown in Figure 1d. Following the very rapid initial decay of the correlation function to zero within 100 fs there is a distinct oscillation between 100 and 200 fs corresponding to the "rebound" of waters against their neighbors followed by subsequent small oscillations; these features are typical of water simulations.[30] At 10 kbar, the time course of the initial decay of the velocity correlation function is the same as that observed at low pressure, while the first oscillation occurs at slightly shorter time. The translational diffusion coefficient of SPC water is calculated from the center of mass mean square displacement to be 2.7×10^{-5} cm^2/s at both 1 bar and 10 kbar. Tse and Klein[29] calculated a decrease in the diffusion coefficient of TIP4P water by 40% at 14 kbar and 340 K, while Stillinger and Rahman found that, for the ST2 water model, there was little change in the diffusion coefficient in simulations of ST2 water at 370 K when the density was increased by up to 36%.[31] The experimental water diffusion coefficient exhibits a complicated pressure–temperature dependence.[32] Up to 313 K, the diffusion coefficient shows an initial increase with pressure to a broad maximum for pressures up to a few kilobar. At higher temperatures, the diffusion coefficient decreases with increasing pressure. It is unclear at present, partly due to the lack of availability of detailed experimental data over a wide enough range of temperatures and pressures, how well the various water models reproduce the anomalous pressure and temperature dependence of the water diffusion coefficient.

B. Pressure Dependence of the Solvation Structure of Formaldehyde. The solvation structure around the formyl end of the molecule is most structured in the ground state and undergoes a large change in solvation upon excitation of the molecule; we analyze specifically the pressure-dependent effects on the solvation of the formyl group in this section. The solvation of the ground state is considered first. The radial distribution functions for the formaldehyde oxygen–water oxygen ($H_2CO(O)$–SPC(O)) atom pair at low and high pressures are shown in Figure 2a. At low pressure, there is a large peak in the distribution function at 2.7 Å. Integration of the first peak to the first minimum (3.25 Å) gives ~2.6 waters in the first solvation shell which are hydrogen bonded to the formyl group. A well-defined second peak at ~4.5 Å is also observed, with approximately 19 water molecules in the

(29) Tse, J. S.; Klein, M. I. *J. Phys. Chem.* **1988**, *92*, 315.
(30) Rahman, A.; Stillinger, F. H. *J. Chem. Phys.* **1971**, *55*, 3336.
(31) Stillinger, F. H.; Rahman, A. *J. Chem. Phys.* **1974**, *61*, 4973.
(32) Woolf, L. A. *J. Chem. Soc., Faraday Trans. 1* **1976**, *72*, 1267.

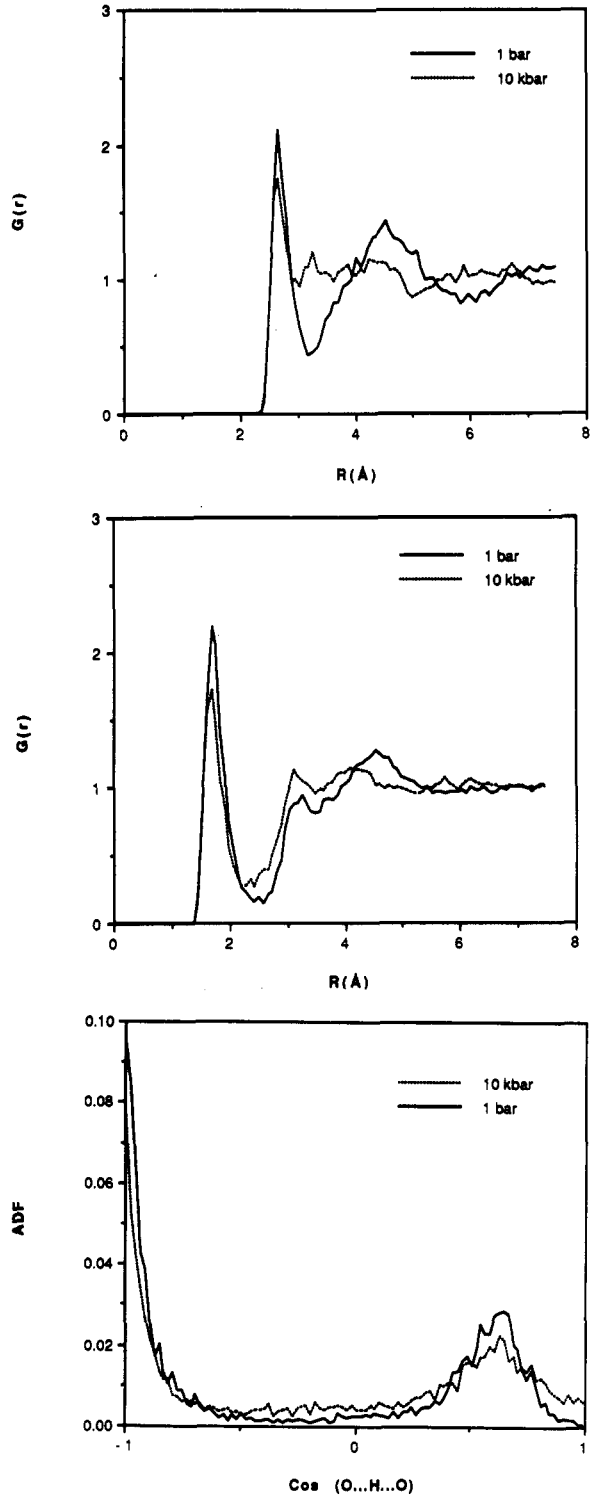

Figure 2. Solute–solvent correlation functions from trajectories with ground-state formaldehyde: (a, top) oxygen–oxygen (formaldehyde–water) radial distribution function at 1 bar and 10 kbar; (b, middle) oxygen–hydrogen (formaldehyde–water) radial distribution function 1 bar and 10 kbar; (c, bottom) oxygen–hydrogen–oxygen (formaldehyde–water–water) at 1 bar and 10 kbar.

second shell.[14b,d] At high pressure, the position of the first peak is unchanged but the height has decreased, and the second peak is largely absent. Integration of the first peak to 3.2 Å gives 2.9 waters in the first solvation shell at high pressure. Note that the number of waters in the first shell increases at high pressure even though the value of the radial distribution function, $g(r)$, at the maximum decreases. This effect arises because $g(r)$ is weighted by the solvent density which is increased by 25% at 10 kbar. The ground-state solute–solvent $^1A_1$ $H_2CO(O)$–SPC(H) radial distribution functions at low and high pressure are shown in Figure 2b. There is a sharp peak at 1.7 Å at both low and high pressure corresponding to hydrogen bonding by solvent to formaldehyde in its ground state. A second peak is observed at low pressure but is largely absent at high pressure. The $H_2CO(O)$–SPC(H)–SPC(O) angular distribution functions at low and high pressure are shown in Figure 2c. The maximum at $\cos\theta_{OHO} = -1$ corresponds to a linear hydrogen bond which is consistent with the peak positions of the solute–solvent O–O and O–H radial distribution functions at 2.7 and 1.7 Å, respectively. The angular distribution of hydrogen bonds from the solvent to the solute at low pressure is essentially unchanged at high pressure (Figure 2c).

TABLE I: Total Solvation Energy (kcal/mol)

	1 bar		10 kbar	
	ground state	excited state	ground state	excited state
$^1A_1$	−26.0	−15.6	−27.0	−15.9
σ	3.8	3.8	3.9	4.1
$^1A_2$	−15.7	−10.4	−16.0	−10.5
σ	2.4	2.2	2.4	2.5
ΔE	10.4	5.2	10.9	5.4
σ	1.8	1.8	1.9	1.9

There are large pressure effects on the solvation structure around the excited-state formaldehyde species. In Figure 3a, the $H_2CO(O)$–SPC(O) radial distribution functions are compared for the 1 bar and 10 kbar simulations. The low-pressure results (Figure 3a) have been discussed previously.[14b] The reduction of the net charge on oxygen from −0.58 e ($^1A_1$) to −0.28 e ($^1A''$) destroys the binding of water molecules to the formaldehyde oxygen at low pressure. This is apparent in Figure 3a where there is a barely noticeable peak at ~3.0 Å dramatically reduced in intensity and moved to larger distance as compared with the ground-state solvation at low pressure shown in Figure 2a. The $H_2CO(O)$–SPC(O) radial distribution function at 10 kbar is also shown in Figure 3a; there is now a very distinct peak in the radial distribution function at 2.9 Å. The first peak is slightly smaller and much broader than the corresponding result for the ground-state species at high pressure. Thus the application of high pressure has induced the formation of a solvation shell around the excited-state molecule. Integration (out to 4.2 Å) of the radial distribution function yields 8.9 waters in the first solvation shell of the excited-state species at high pressure. The excited-state solute–solvent $^1A''$ $H_2CO(O)$–SPC(H) radial distribution functions at low and high pressure are shown in Figure 3b and the $H_2CO(O)$–SPC(H)–SPC(O) angular distribution functions at low and high pressure are shown in Figure 3c. Although the reduced electronegativity of the formyl group does not support a distinct solvation shell at low pressure, waters at the surface do tend to have their hydrogens oriented toward the formaldehyde oxygen. This is most apparent in the $H_2CO(O)$–SPC(H)–SPC(O) angular distribution function (Figure 3c) which at low pressure has a maximum at $\cos\theta_{OHO} = -1$, corresponding to a linear hydrogen bond to the solute. In contrast, at high pressure (Figure 3c) the solvation shell waters around the excited-state species ($^1A_2$) have rotated their OH bond by ~180°, and waters in the first solvation shell are no longer hydrogen bonded to the solute (see Figure 3c). Thus, at high pressure, although both the ground $^1A_1$ and the excited $^1A''$ states have a well-defined solvation shell, the angular orientations of waters in these shells are very different for the two states.

C. Pressure Effects on the Energetics of Solvation. In Table I we report the average solute–solvent interaction (solvation) energy and solvation energy differences corresponding to four different simulations: those with solvent equilibrated around the ground state and excited state solute at low and high pressure, respectively. The solvation energy differences listed in the third row correspond to classical estimates of the absorption and long time fluorescence line shifts. For example, the results listed in the first column correspond to a simulation in which the solvent "feels" the solute in its ground state; i.e., the ground-state potential parameters are used for the solute during the simulation. The simulation was run at 1 bar pressure. The results listed in the

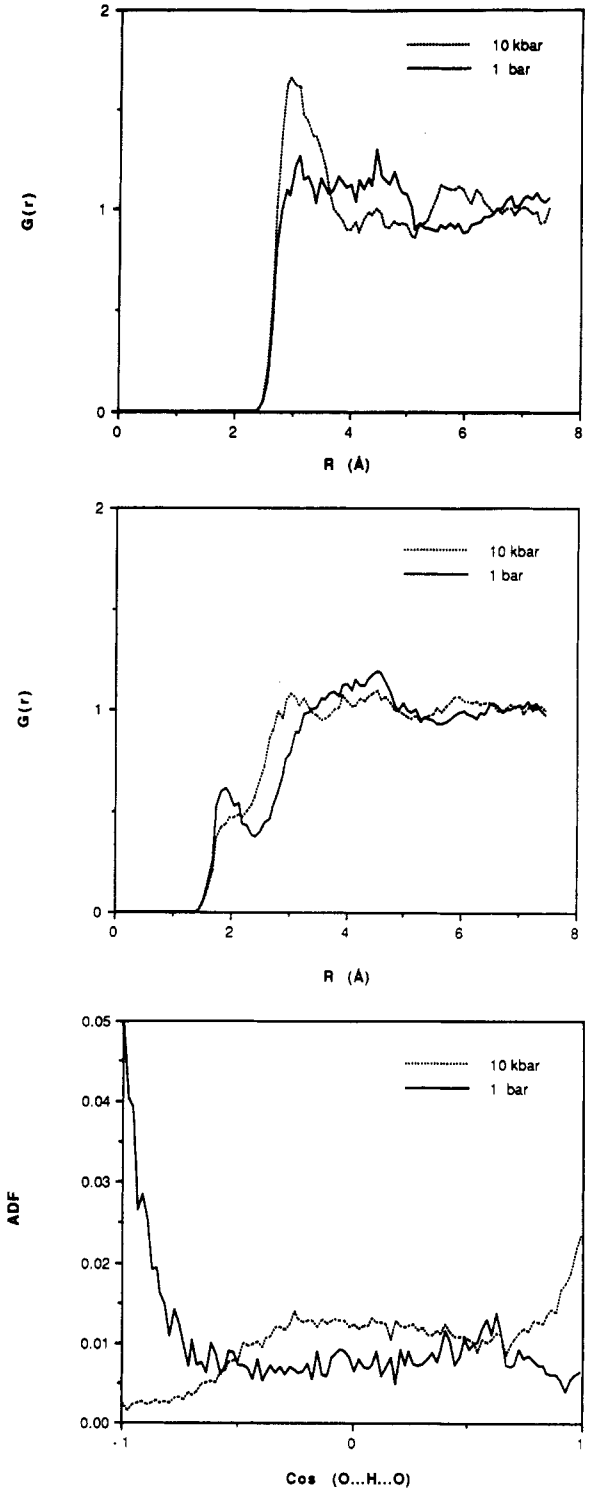

Figure 3. Solute–solvent correlation functions from trajectories with excited state formaldehyde: (a, top) oxygen–oxygen (formaldehyde–water) radial distribution function at 1 bar and 10 kbar; (b, middle) oxygen–hydrogen (formaldehyde–water) radial distribution function at 1 bar and 10 kbar; (c, bottom) oxygen–hydrogen–oxygen (formaldehyde–water–water) at 1 bar and 10 kbar.

second column correspond to a simulation in which the excited-state potential parameters were used for the solute during the simulation. The simulation was run at 1 bar pressure. Columns 3 and 4 list the corresponding results at 10 kbar. The solvation energy of the solute in the ground state interacting with solvent equilibrated around the ground state is −26.0 ± 3.8 kcal/mol (first row and first column, Table I). It is possible to use this simulation to estimate the absorption line shift due to solvent. To make this estimate, at each configuration in the trajectory the solute–solvent interaction energy is computed with the solute excited-state potential parameters (partial charges and Lennard-Jones parameters) substituted for the ground-state values.[14] Thus the average solvation energy of the excited $^1A''$ state solute interacting with solvent equilibrated around the ground state is −15.7 ± 2.4 kcal/mol (third row and first column, Table I). If the difference between the solvation energy of the ground and excited states is averaged over a trajectory created with ground-state solute parameters, the solvent-induced absorption line shift can be computed (10.4 ± 1.8 kcal/mol; fifth row and first column, Table I). Thus, at low pressure, the solvent-induced absorption blue shift is calculated to be 10.4 kcal/mol while the long-time fluorescence blue shift calculated from a separate simulation with solvent equilibrated around the solute in the excited state is computed to be 5.2 kcal/mol. The peak in the emission spectrum is thus red-shifted with respect to the absorption spectrum due to solvent relaxation.[14] The solvent shifts calculated from the high-pressure simulations shown in Table I (row five, columns three and four) are very close to the shifts calculated from the low-pressure simulations. At high pressure, the solvent-induced absorption blue shift is calculated to be −10.9 ± 1.9 kcal/mol, while the long-time fluorescence blue shift is 5.4 ± 1.9 kcal/mol. The difference between the solvent contributions to the simulated optical absorption energy at low pressure (10.4 kcal/mol) and high pressure (10.9 kcal/mol) leads to a predicted pressure-induced blue shift that is very small ~0.5 kcal/mol (165 cm^{-1}) at 10 kbar. It is of interest to note that the solvent contributions to the absorption line widths are given by the standard deviations in the transition energies listed in the last row of Table I. The increase in pressure up to 10 kbar has a negligible effect on the calculated line widths.

It is surprising that the pressure effects on the solvent line widths are so small in view of the relatively large pressure-induced changes in the solute–solvent structure, particularly for the excited state discussed in the previous section. From Table I it is apparent that the *total* molecular solvation energies of the ground-state and excited-state species exhibit very small changes with pressure up to 10 kbar. In Table II we list the partial atomic solvation energies of each of the solute atomic centers (C, O, H1, H2) from the four simulations. It is clear that there are pressure-induced changes in the solvation energies of the individual atomic centers but that the changes tend to cancel. The application of pressure decreases the solvation energy of the formyl oxygen for both the ground-state and excited-state species while the solvation energy of the formaldehyde hydrogens increases. The partial atomic solvation energy changes listed in Table II can be rationalized qualitatively in terms of the pressure effects on the solute–solvent distribution functions discussed in the previous section. The partial atomic solvation energy of the formyl oxygen in the ground state is calculated to be −22.2 kcal/mol at 1 bar and −18.9 kcal/mol at 10 kbar when a 7.5-Å solute–solvent cutoff is used to calculate the atomic solvation energy (see Table II). However, when only the first solvation shell of the formyl oxygen is used (3.2-Å solute–solvent cutoff) to calculate the solvation energy of this atom, the partial

TABLE II: Partial Atomic Solvation Energy of $^1A_1$ Formaldehyde and $^1A''$ Formaldehyde

	solvation energy,[a] kcal/mol	
	1 bar	10 kbar
A. $^1A_1$ Formaldehyde		
FMO	−22.2	−18.9
FMC	−0.8	−3.5
FMH1	−1.5	−2.3
FMH2	−1.5	−2.3
total	−26.0	−27.0
B. $^1A''$ Formaldehyde		
FMO	−4.7	−3.6
FMC	−1.5	−1.3
FMH1	−2.1	−2.8
FMH2	−2.1	−2.8
total	−10.4	−10.5

[a] Solvation energy includes waters within 7.5-Å cutoff from formaldehyde oxygen.

atomic solvation energy of the formyl oxygen is very close to the same value (~18.5 kcal/mol) at both low and high pressure as expected from the very small changes in the distribution functions with pressure shown in Figure 2. As for the excited state, the partial solvation energy of the formyl oxygen is calculated to be −4.7 kcal/mol at 1 bar and decreases to −3.6 kcal/mol at 10 kbar (Table II). When only the first solvation shell is included in the calculation, however, the partial solvation energy becomes even less attractive at higher pressure (−4.0 kcal/mol at 1 bar versus −2.4 kcal/mol at 10 kbar). This is consistent with the structural results shown in Figure 3 which suggest that the pressure-induced changes in the solvation shell of the formyl oxygen lead to more repulsive interactions.

In summary, we find that the very small changes in the *total* solvation energies do not reflect the larger pressure-induced changes in the solvation shell of this model dipolar solute because of the cancellation of contributions from changes in the solvation of the positive and negative atomic centers. The cancellation is to some extent a consequence of the fact that waters in the first shell which are oriented so as to interact favorably with the negative atomic centers will have a repulsive interaction with the positive centers and vice versa.

D. Pressure Effects on the Time Dependence of the Solvation Response. The equilibrium simulations of formaldehyde with ground-state or excited-state potential parameters correspond to the end points of time-resolved studies of the solvent response following the simulation of an optical excitation of the solute. The time dependence of the nonequilibrium solvation response at low pressure was discussed previously.[14d] Summarizing the results at low pressure, the fluorescence shift and solvation relax nonexponentially on a very fast time scale. The major portion of the relaxation occurs within 100 fs, with additional relaxation observed up to 1 ps. The contributions of different solvent shells to the relaxation were analyzed and the time-dependent changes in solute–solvent radial distribution functions evaluated. The major portion of the relaxation was attributed to translational motions of the first solvation shell. In the present work we have carried out further analysis at both low and high pressure to compare the nonequilibrium response function with equilibrium correlation functions of solvation energy fluctuations. The equilibrium and nonequilibrium response functions are

$$C(t)_{\text{equilib}} = \langle \Delta E(t)\Delta E(0)\rangle / \langle \Delta E(0)\Delta E(0)\rangle \quad (1)$$

$$C(t)_{\text{nonequilib}} = [\langle E_{\text{A''-solvent}}(t) - E_{\text{A1-solvent}}(0)\rangle]/[\langle E_{\text{A''-solvent}}(\infty) - E_{\text{A1-solvent}}(0)\rangle] \quad (2)$$

where for the nonequilibrium response corresponding to a fluorescence experiment, the brackets $\langle\ \rangle$ indicate an ensemble average of trajectories with the solute potential switched from the ground to the excited state at time zero. For the equilibrium response function, the fluctuations in solvation energy $\Delta E(t)$ are to be carried out with a fixed solute potential, i.e., for the fluctuations on the ground-state surface $\Delta E(t) = E_{\text{A1-solvent}}(t) - \langle E_{\text{A1-solvent}}\rangle$. Figure 4 compares the nonequilibrium solvation response function at high pressure with the equilibrium correlation functions calculated from separate simulations with solute in the ground state in one simulation and in the excited state in another. The three curves are remarkably similar. These results demonstrate that the nonequilibrium response for this system is predicted by linear response theory to a surprising degree of accuracy; similar results have been reported by others studying ionic systems.[11,33,39] The general features of the equilibrium and nonequilibrium response functions are very similar at low pressure (not shown). It is surprising that the solvation energy–time correlation functions appear so similar for the different conditions studied (there are six different simulations corresponding to the low- and high-pressure simulations of the following: solvent dynamics in equilibrium with the ground state; solvent dynamics in equilibrium with the excited state; nonequilibrium solvent response to an excitation). The small size of the solute and the R^{-3} dependence

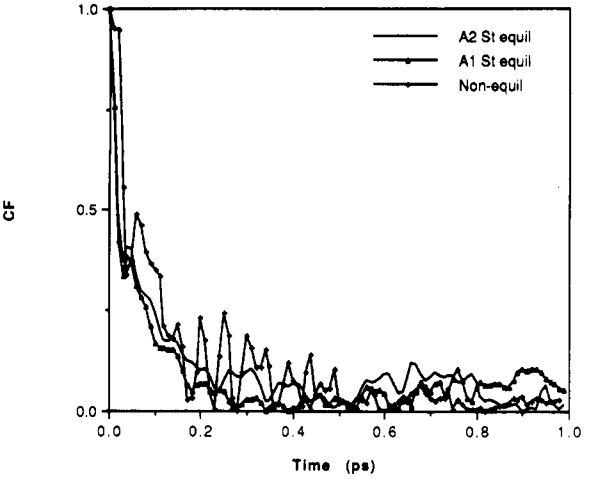

Figure 4. Solvation response functions at 10 kbar: nonequilibrium response function following a simulated excitation of formaldehyde from the ground $^1A_1$ state to the excited $^1A''$ state, see text, eq 1; equilibrium correlation functions from trajectories with formaldehyde in the ground state, and in the excited state.

of the solute–solvent dipolar coupling weights relaxation from the first solvation shell heavily and favors translational relaxation modes. Each of the correlation functions appears to have an identical initial component of the decay (about 50% of the total) lasting ~20 fs; this component reflects the quasi free motion of the solvent over very short distances and times as opposed to restructuring of the solvation shell. At latter times, the behavior of the response functions is more complicated, since the nonequilibrium dynamics must reflect the restructuring of the solvation shell as well as other relaxation modes (rotational motions of more distant solvent molecules). The persistent high-frequency oscillations observed in the time correlation functions probably reflect librational motions of the solvation shell. At high pressure, the high-frequency oscillations of the nonequilibrium response function appear to be accentuated (compare Figure 4 with Figure 1 in ref 14d).

As discussed above, at high pressure the solvation shell surrounding the formyl group remains largely intact following the excitation, although the solute–solvent O–O peak moves out somewhat and broadens. Also at high pressure, the rotational orientation of the waters in this shell changes by ~180° following the excitation. In Figure 5 we plot the angular distribution function for first shell waters at various times following the simulated excitation. The rotational reorganization of the solvent shell at high pressure is more than an order of magnitude slower than the rotational relaxation at low pressure. While the hydrogen bonding to the solute of these waters is destroyed within 100 fs, it takes longer than 2 ps to fully establish the new orientational structure of the solvation shell waters that is observed in the equilibrium simulations of the solvated excited-state species. Evidently this rearrangement must involve more extensive interactions with, and hydrogen bonding to, additional solvent molecules beyond the first shell.

Concluding Remarks: Molecular Mechanisms of Pressure Tuning Spectroscopy

The perturbation of electronic energy levels of a chromophore by the application of high pressures in liquids and solids has been named "pressure tuning spectroscopy" by Drickamer.[34,35] There are three important mechanisms by which a change in the pressure can perturb the electronic energy spacing. The compression of bonds can increase the energy spacing between bonding and antibonding orbitals, leading to a blue shift; this is an intramolecular effect. The compression of the spacing between molecules and/or changes in the solvation shell structure can affect both the dis-

(33) Bader, J.; Chandler, D. *Chem. Phys. Lett.* **1989**, *157*, 501.

(34) Drickamer, H. G. *Annu. Rev. Phys. Chem.* **1982**, *33*, 25.

(35) Drickamer, H. G. In *AIP Conference Proceedings #190*; American Institute of Physics: New York, 1988; p 101.

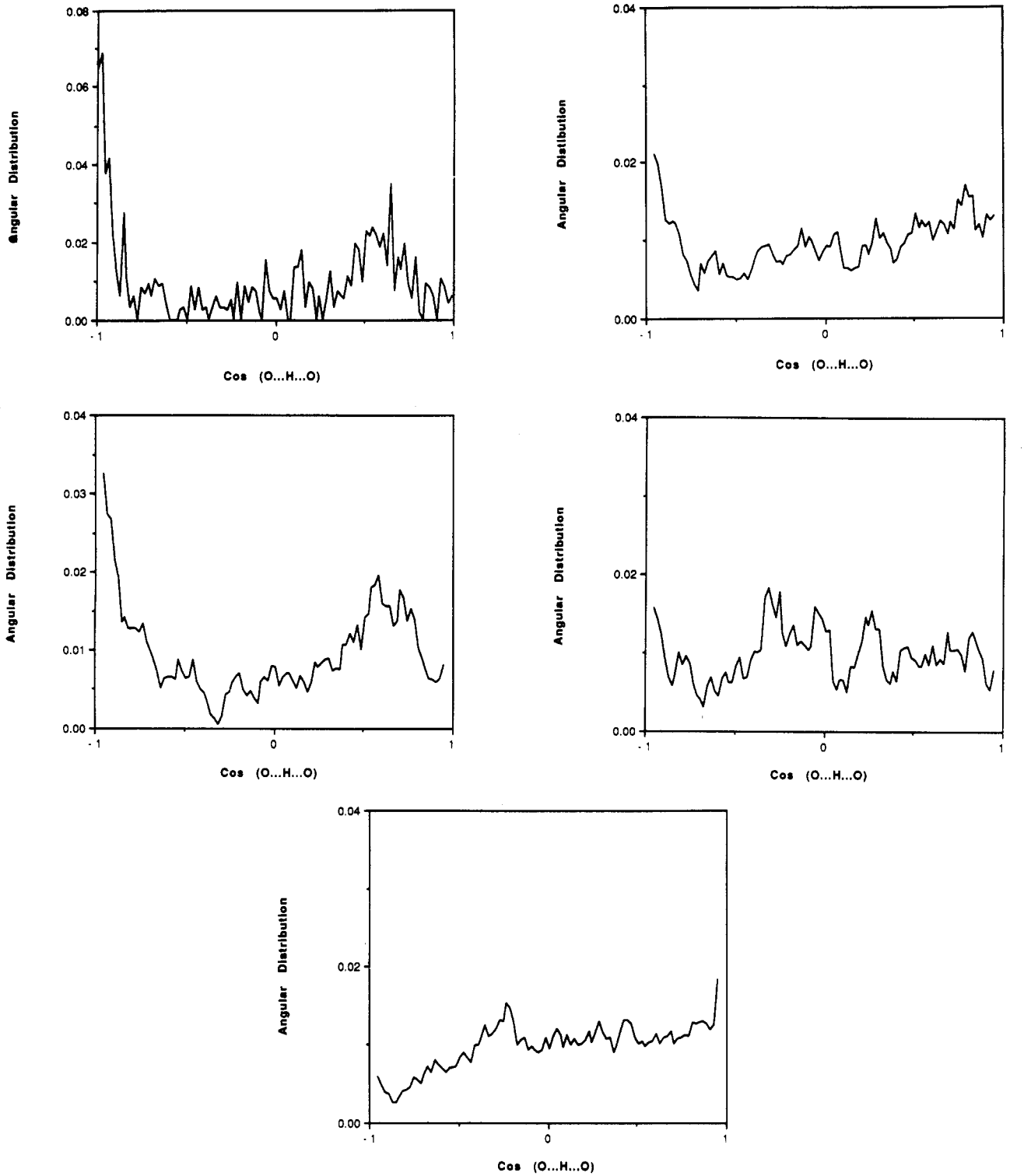

Figure 5. Time evolution of the O–H–O (formaldehyde–water–water) angular distribution function following the excitation at high pressure, 10 kbar: (a, top left) t = 0 fs (ground-state angular distribution function); (b, middle left) t = 20 fs; (c, top right) t = 200 fs; (d, middle right) t = 1500 fs; (e, bottom) t = 2500 fs.

persion and dielectric interactions, leading to either a blue shift or a red shift; this is an intermolecular effect. In principle, the molecular mechanics parametrization of the solute ground- and excited-state surfaces of the kind used in the present study or mixed quantum/classical simulations of the kind we used previously to simulate solvent effects on optical absorption[14b] could be used to evaluate the influence of pressure on bond compression and the energy gap. We do observe a very small decrease ($\sim 10^{-3}$ Å) in the average CO bond length for both the ground- and excited-state species at 10 kbar. The compression is much smaller that the rms fluctuation ($\sim 10^{-2}$ Å) of the CO bond. The other internal coordinates, particularly the "soft" out-of-plane vibration, should be more sensitive to applied pressures in the range $\sim$10 kbar. However, we have not analyzed these effects as we expect that the pressure range employed in the simulations is too limited to observe significant distortion of molecular geometries. Also, we have not reparametrized the van der Waals dispersion coefficient for the $^1A''$ excited state of formaldehyde. The promotion of an electron from a localized lone pair to a diffuse π^* orbital will increase the polarizability of the molecule and therefore increase its dispersion interactions with the solvent. Pressure effects on optical spectra attributed to polarizability changes in the chromophore upon excitation have been observed at very high pressures, i.e., those exceeding 100 kbar.[36] For a model solute like

formaldehyde, which has a large change in the dipole moment in going from the $^1A_1$ to the $^1A''$ state, dissolved in a highly polar solvent like water, it is expected that pressure-induced changes in the dipolar interactions between the chromophore and solvent will dominate other intramolecular or intermolecular effects.

The relatively large pressure-induced changes we observed in the solvation shell structure in the $^1A''$ state are not reflected in the solvation energetics. We attribute this to compensation of the more repulsive interactions of the formyl group with solvent at high pressure by the increased attraction between the centers of positive charge (formaldehyde protons) and the water. The present simulation of pressure-induced effects on solvation structure and energetics of formaldehyde in water complements our recent studies of solvation effects on the absorption and fluorescence of this model dipolar solute.[14b,d] Our results concerning the pressure effects on the solvation of formaldehyde by water suggest that, even for as simple a solute as formaldehyde, it is important to account for the extended (nonspherical) shape and charge distribution of the solute as well as the molecular details of the solvation shell in developing molecular models for pressure effects on spectra.

Pressure tuning spectroscopy has recently been applied to study the absorption spectra of binuclear complexes.[37] These mixed valence compounds are used to study intramolecular electron transfer and continuum models have been applied to interpret solvent effects on their spectra.[38] The fundamental result of the pressure studies is that no shifts in the intervalence electronic absorption band were observed following pressure-induced freezing of the solvent, whereas continuum solvent models predicted large shifts due to the decrease in solvent dielectric constant upon freezing. To account for these results, it was suggested that the metal ligands together with a relatively rigid solvation shell could shield the solvent dielectric effects. Molecular simulations of these mixed valence systems should provide a powerful tool to analyze the pressure-induced changes in the solvation shell and the effects of the solvation shell on electron-transfer dynamics and spectra.

Acknowledgment. This work has been supported in part by National Institutes of Health grant GM-30580. D.B.K. and M.B. have been supported in part by Supercomputer Postdoctoral Fellowships from the New Jersey Commission on Science and Technology. D.B.K. is the recipient of a National Institutes of Health NRSA fellowship. We thank David Kofke for implementing the constant pressure simulation method within the IMPACT program. We also acknowledge grants of supercomputer time from the John Von Neumann Center and the Pittsburgh Supercomputer Center.

(36) Mitchell, D. J.; Drickamer, H. G.; Schuster, G. B. *J. Am. Chem. Soc.* **1977**, *99*, 7489.
(37) Hammack, W. S.; Drickamer, H. G.; Lowery, M. D.; Hendrickson, D. N. *Inorg. Chem.* **1988**, *27*, 1307.
(38) (a) Powers, M. J.; Meyer, T. J. *J. Am. Chem. Soc.* **1980**, *102*, 1289. (b) Hammack, W. S.; Drickamer, H. G.; Lowery, M. D.; Hendrickson, D. N. *Chem. Phys. Lett.* **1986**, *132*, 231.
(39) Note Added in Proof: The breakdown of linear response theory for the nonequilibrium solvation response to a large dipole moment change of a solute in methanol has recently been reported. Fonseca, T.; Ladonyi, B. M. *J. Phys. Chem.*, submitted for publication.

Staggered and Doubly Bridged B_2H_4: Computational Evaluation of Their Temperature Interplay[1]

Zdeněk Slanina[2]

Max-Planck-Institut für Chemie (Otto-Hahn-Institut), D-6500 Mainz, Federal Republic of Germany
(Received: August 1, 1990)

A computational evaluation of relative stabilities of staggered D_{2d} and double-bridged C_{2v} isomers of B_2H_4 in the ideal gas phase has been carried out on the basis of recent quantum chemical data. The possibility is indicated that after surpassing the temperature threshold not much above room temperature, the global energy minimum becomes a less significant component of the isomeric mixture. A quite close coexistence of both structures or predominance of the D_{2d} isomer at moderate temperatures is predicted. Also characterized are the temperature maxima of the heat capacity term originated from this isomeric interplay.

Introduction

Lively theoretical interest in various aspects of borane chemistry has been evoked recently (see, e.g., refs 3-9), which in particular is true of the B_2H_4 species.[10-20] Much more is known about this system from calculations than from observation.[21] A distinct structural phenomenon connected with this species is its isomerism, namely, the existence of (at least) two local energy minima at its

(1) Dedicated to Professor Paul von Ragué Schleyer on the occasion of his 60th birthday.
(2) The permanent and reprint order address: The J. Heyrovský Institute of Physical Chemistry and Electrochemistry, Czechoslovak Academy of Sciences, Dolejškova 3, CS-18223 Prague 8-Kobylisy, Czech and Slovak Federal Republic.
(3) DeFrees, D. J.; Raghavachari, K.; Schlegel, H. B.; Pople, J. A.; Schleyer, P. v. R. *J. Phys. Chem.* **1987**, *91*, 1857.
(4) Curtiss, L. A.; Pople, J. A. *J. Chem. Phys.* **1989**, *91*, 4809.
(5) Curtiss, L. A.; Pople, J. A. *J. Chem. Phys.* **1989**, *91*, 4189.
(6) McKee, M. L. *J. Phys. Chem.* **1989**, *93*, 3426.
(7) Stanton, J. F.; Lipscomb, W. N.; Bartlett, R. J. *J. Am. Chem. Soc.* **1989**, *111*, 5165.
(8) Stanton, J. F.; Lipscomb, W. N.; Bartlett, R. J. *J. Am. Chem. Soc.* **1989**, *111*, 5173.
(9) Schleyer, P. v. R.; Bühl, M.; Fleischer, U.; Koch, W., to be published.
(10) Blustin, P. H.; Linnett, J. W. *J. Chem. Soc., Faraday Trans. 2* **1975**, *71*, 1058.
(11) Dill, J. D.; Schleyer, P. v. R.; Pople, J. A. *J. Am. Chem. Soc.* **1975**, *97*, 3402.
(12) Armstrong, D. R. *Inorg. Chim. Acta* **1976**, *18*, 13.
(13) Pepperberg, I. M.; Halgren, T. A.; Lipscomb, W. N. *Inorg. Chem.* **1977**, *16*, 363.
(14) Bigot, A. B.; Lequan, R. M.; Devaquet, A. *Nouv. J. Chem.* **1978**, *2*, 449.
(15) McKee, M. L.; Lipscomb, W. N. *J. Am. Chem. Soc.* **1981**, *103*, 4673.
(16) Vincent, M. A.; Schaefer, H. F. *J. Am. Chem. Soc.* **1981**, *103*, 5677.
(17) Mohr, R. R.; Lipscomb, W. N. *Inorg. Chem.* **1986**, *25*, 1053.
(18) Stanton, J. F.; Lipscomb, W. N.; Bartlett, R. J. In *Boron Chemistry. Proceedings of the 6th International Meeting on Boron Chemistry*; Heřmánek, S., Ed.; World Scientific Publ. Comp.: Singapore, 1987; pp 74-82.
(19) Curtiss, L. A.; Pople, J. A. *J. Chem. Phys.* **1989**, *90*, 4314.
(20) Curtiss, L. A.; Pople, J. A. *J. Chem. Phys.* **1989**, *91*, 5118.
(21) Ruščic, B.; Schwarz, M.; Berkowitz, J. *J. Chem. Phys.* **1989**, *91*, 4576.

0022-3654/91/2095-1089$02.50/0